Published in final edited form as:
Proteomics. 2010 December ; 10(24): 4415–4430. doi:10.1002/pmic.201000298.

Plasma profiles in active systemic juvenile idiopathic arthritis: biomarkers and biological implications

Xuefeng B. Ling[1,5,*], **Jane L. Park**[1,6,*], **Tanya Carroll**[1,5], **Khoa D. Nguyen**[1], **Kenneth Lau**[1,5], **Claudia Macaubas**[1,6], **Edward Chen**[1,5], **Tzielan Lee**[1], **Christy Sandborg**[1], **Diana Milojevic**[2], **John T. Kanegaye**[3], **Susanna Gao**[1], **Jane Burns**[4], **James Schilling**[1,5], and **Elizabeth D. Mellins**[1,6,*]

[1]Department of Pediatrics, Stanford University, Stanford, CA 94305

[2]Department of Pediatrics, University of California San Francisco, San Francisco, CA 94143

[3]Department of Emergency Medicine, University of California School of Medicine and Rady Children's Hospital San Diego, San Diego, La Jolla, CA 92093

[4]Department of Pediatrics, University of California San Diego School of Medicine, La Jolla, CA 92093

[5]Pediatric Biotechnology Core, Stanford University, Stanford, CA 94305

[6]Program in Immunology, Stanford University, Stanford, CA 94305

Abstract

Systemic juvenile idiopathic arthritis (SJIA) is a chronic arthritis of children characterized by a combination of arthritis and systemic inflammation. There is usually nonspecific laboratory evidence of inflammation at diagnosis but no diagnostic test. Normalized volumes from 89/889 2D protein spots representing 26 proteins revealed a plasma pattern that distinguishes SJIA flare from quiescence. Highly discriminating spots derived from 15 proteins constitute a robust SJIA flare signature and show specificity for SJIA flare in comparison to active polyarticular juvenile idiopathic arthritis (poly JIA) or acute febrile illness (FI). We used 7 available ELISA assays, including one to the complex of S100A8/S100A9, to measure levels of 8 of the15 proteins. Validating our DIGE results, this ELISA panel correctly classified independent SJIA flare samples, and distinguished them from acute febrile illness. Notably, data using the panel suggest its ability to improve on ESR or CRP or S100A8/S100A9, either alone or in combination in SJIA F/Q discriminations. Our results also support the panel's potential clinical utility as a predictor of incipient flare (within 9 weeks) in SJIA subjects with clinically inactive disease. Pathway analyses of the 15 proteins in the SJIA flare versus quiescence signature corroborates growing evidence for a key role for IL-1 at disease flare.

Keywords

Systemic Juvenile Idiopathic Arthritis; Kawasaki Disease; 2D-DIGE (two-dimensional difference in gel electrophoresis); MALDI-TOF/TOF MS (matrix-assisted laser desorption/ionization time of flight mass spectrometry); Proteomic profile

[*]Correspondence: Elizabeth D. Mellins, Department of Pediatrics, Stanford University, 259 Campus Drive, Stanford, CA 94305-5164, mellins@stanford.edu.
[*]These authors contributed equally to this work.

INTRODUCTION

Juvenile idiopathic arthritis (JIA) is an umbrella term encompassing a group of seven clinically distinguishable subtypes, all characterized by chronic inflammatory arthritis [1]. Taken together, the JIA subtypes constitute the most common pediatric rheumatic condition. Polyarticular JIA (poly JIA) includes two subtypes (rheumatoid factor positive (RF+) and the more common RF negative (RF−), with the RF+ subtype resembling adult rheumatoid arthritis. Systemic juvenile idiopathic arthritis (SJIA) is a JIA subtype uniquely characterized by a combination of systemic features and arthritis. Its course is persistent or polycyclic with periods of disease flare and quiescence in about 60% of affected subjects [2]; approximately 40% experience a monocyclic course that resolves [2]. Unlike other JIA subtypes, adaptive immune responses appear to play a limited role in SJIA, whereas excessive innate immune responses are prominent [3]. Among the seven JIA subtypes, SJIA has the worst prognosis in terms of disease complications, treatment response, and mortality [4–7].

The etiology of SJIA is unknown, and there are no diagnostic tests. Laboratory markers of active disease in SJIA include the erythrocyte sedimentation rate (ESR) and C-reactive protein (CRP), but these tests do not discriminate SJIA from other inflammatory conditions. Initial differential diagnosis of SJIA can be difficult, and it remains a significant clinical challenge to differentiate SJIA flare from other causes of fever such as malignancy, infection, other autoimmune disease, Kawasaki disease, and other inflammatory disorders. Furthermore, changes in clinical laboratory tests are noted concurrently with other clinical evidence of flare, but do not serve as biomarkers of impending flare. Such predictive markers would likely be of value; indeed, evidence that early treatment of flare is beneficial and reduces disease complications has been presented for RA [8]. In addition to informing clinical care, plasma protein features that correlate with SJIA disease activity might shed light on disease pathogenesis.

In light of these considerations, there is strong rationale for efforts to discover diagnostic and prognostic biomarkers in SJIA. Among the plasma proteins that have been suggested as candidate biomarkers of active SJIA are calcium-binding proteins S100A12, the product of activated granulocytes, and the S100A8/S100A9 complex (calprotectin), secreted by activated granulocytes, monocytes and immature macrophages, and inducible In mature macrophages, osteoclasts and keratinocytes [9–13]. Another candidate is IL-18, a pro-inflammatory cytokine that rises to markedly high circulating levels during SJIA flare [14, 15]. Serum amyloid A (SAA), an acute phase protein, also was identified as an SJIA disease activity marker in a discovery effort using SELDI-TOF MS analysis of plasma [16]. In Adult Still's disease, the adult homologue of SJIA, high levels of ferritin are characteristic [17], and procalcitonin levels may help discriminate inter-current bacterial infection from non-infectious inflammation [18–20]. However, both S100A12 as a marker of SJIA compared to infection and PCT as a marker of infection compared to active inflammatory disease are limited by relatively low sensitivity (~65%) [10, 19, 20].

The need for more robust biomarkers in SJIA led us to take a proteomic approach to biomarker discovery in plasma, the most comprehensive human proteome. We hypothesized that there would be differential plasma proteomic signatures reflective of SJIA disease flare and quiescence, detectable using two-dimensional difference gel electrophoresis (2D-DIGE). This proved to be the case. To explore the specificity of the plasma protein biomarkers for the inflammatory state in SJIA, we evaluated flare/quiescence differential 2D-DIGE profiles in samples from individuals with polyarticular JIA, acute febrile illness (FI), and Kawasaki Disease (KD), a systemic inflammatory disease complicated by coronary artery aneuryms [21]. This analysis revealed heterogeneity in the acute phase response

across the conditions we evaluated. Based on the candidate SJIA flare biomarkers suggested by 2D-DIGE, we tested a panel of 7 ELISAs, a higher throughput method, to validate our findings. We investigated the hypothesis that molecular changes detected by this panel occur in advance of clinical SJIA flare. We also used pathway analysis of the proteins altered during active SJIA to reveal clues to disease mechanisms.

EXPERIMENTAL PROCEDURES

The overall data analysis and sample allocation steps are illustrated in Supplementary Figure 1.

Clinical variables and scoring system

Comprehensive clinical and clinical laboratory data on children with JIA were collected in association with each plasma sample. All children with juvenile arthritis fulfilled the criteria of the International League of Associations for Rheumatology (ILAR) criteria for JIA [22]. For SJIA subjects, the presence or absence of clinical features such as fever, rash, serositis, and macrophage activation syndrome (MAS) was documented at each visit. Clinical laboratory data such as erythrocyte sedimentation rate (ESR), platelets, white blood cell count (WBC), C-reactive protein, ferritin, and d-dimer were documented at most visits. We used the aforementioned clinical features and laboratory data as measures of systemic activity in SJIA subjects. In addition, the presence or absence of arthritis was documented in both SJIA and polyarticular JIA (poly JIA) subjects. For SJIA subjects, a systemic flare sample was defined as having any one of the above clinical features or any abnormal laboratory value. For both SJIA and poly JIA subjects, an arthritis flare sample was defined as having arthritis in one or more joint(s). Therefore, poly JIA flare samples were based on the presence of arthritis alone, while SJIA flare samples were based on the presence of arthritis and/or systemic features of flare. The presence of arthritis was determined by a pediatric rheumatologist and required either joint swelling or joint pain with limitation of motion. The SJIA flare samples used in our studies were taken from patients with systemic and arthritis flare features with the exception of one sample used in our 2D-DIGE analysis which had systemic features of disease only. The intensity of a flare sample was also measured and was based on a scoring system that we developed as a means to grade severity of systemic disease manifestations and arthritis and to facilitate correlation between clinical and proteomic data. (Supplementary Table 1A/B/C). Active disease was defined as a flare sample and was broken into two components: arthritis scores were assigned by a pediatric rheumatologist, who reviewed the medical record, including clinical laboratory data. The systemic scoring (Supplemental Table 1A) is based on the results of hierarchical clustering analysis of SJIA subjects with early (<3 months) active disease [23]. Arthritis scoring (Supplemental Tables 1B, 1C) is based on the number of “active” joints, defined as swelling or limitation of motion with pain in an affected joint. The scoring of arthritis severity is different for SJIA and poly JIA subjects, because the patterns of joint involvement are different between the 2 groups [1, 4]. The scoring is based on differences in frequency analysis of numbers of active joints in early active SJIA compared to active poly JIA ([23] and C. Sandborg, unpublished data). For the purpose of this study, we defined a flare sample as one with a systemic score greater than 0 and an arthritis score > A (SJIA subjects) or > 0 (poly JIA subjects). A quiescent sample was defined as one with a systemic score of 0 or an arthritis score of A (SJIA) or 0 (poly JIA). The majority of SJIA flare samples used in our studies had systemic scores of 1 or 2 and arthritis scores of B and C. The poly JIA flare samples in our studies had a range of arthritis scores from 1 to 3.

Study subjects

Protocols for this study were approved by the institutional review boards at the clinical centers, and all parents gave written consent for the participation of their child. Child and adolescent assent were obtained as appropriate. Children with SJIA and poly JIA were recruited from the Pediatric Rheumatology Clinics at Lucile Packard Children's Hospital, Stanford, California, USA from 2000 to 2008 and at the University of California, San Francisco (UCSF) from 2006 to 2008. Serial peripheral blood samples were collected from these subjects, including samples from periods of active disease noted as flare (F) and inactive disease noted as quiescence (Q). Comprehensive clinical data were also collected from these subjects. We studied 10 SJIA subjects with paired F and Q samples by 2D-DIGE. 9 of 10 SJIA F samples used in our 2D-DIGE analysis were from subjects with both active arthritis and systemic disease activity; the remaining subject had only active systemic features without clinically detectable arthritis. For the ELISA analysis, we used matched F/Q samples from 18 SJIA subjects (9/18 subjects also provided samples for the 2D-DIGE analysis) and samples from 4 additional subjects at F and 4 additional (unmatched) subjects at Q. As serial samples were available on most subjects, there was only 1 SJIA F sample and 5 SJIA Q samples used in both ELISA and DIGE studies. To construct training and testing F and Q cohorts for ELISA analyses, all samples were randomized with the consideration that similar portions of the samples are matched F/Q in training and testing sets (5 subjects, 10/24, 41.2% samples and 4 subjects, 8/20, 40% samples, respectively). 15 SJIA subjects contributed Q samples in the prediction of flare ELISA experiment; no samples in this analysis were used in any other assay. We also studied 5 poly JIA subjects with paired F and Q samples by 2D-DIGE. For the ELISA analysis, we used matched F/Q samples from 15 poly JIA subjects (2/15 also provided samples for the 2D-DIGE analysis) and samples from 8 additional poly JIA subjects at F. There were matched F/Q samples from 2 Poly JIA subjects and 1 Poly JIA F sample (unmatched) used in both ELISA and DIGE studies. Clinical and demographic characteristics of JIA subjects included in the study are summarized in Supplementary Tables 2A/B, 3A/B and 4.

For KD and FI samples, subjects who presented to the Emergency Department at Rady Children's Hospital San Diego and met study criteria were enrolled from 2004 to 2008. Inclusion criteria for children with KD were 4 out of 5 standard clinical criteria (rash, conjunctival injection, cervical lymphadenopathy, changes in the extremities, changes in the oropharynx) or 3 of 5 criteria with dilated coronary arteries by echocardiogram. All KD patient samples were taken prior to intravenous immunoglobulin (IVIG) treatment. Inclusion criteria for the other febrile children were fever for at least 3 days accompanied by any of the following signs: rash; conjunctival injection; cervical lymphadenopathy; oropharyngeal erythema; or peripheral edema. Enrolled subjects were ultimately found to have the following diagnoses: SJIA, scarlet fever, viral syndrome, staphylococcal abscess (methicillin-resistant and methicillin-sensitive), streptococcal adenitis, bacterial urinary tract infection, viral meningitis, perirectal abscess, and Henoch Schonlein purpura (HSP). Clinical and demographic characteristics of KD and FI subjects included in the study are summarized in Supplementary Tables 2B and 3B. Each subject provided a single blood sample at study enrollment. There was no overlap between the KD and FI subjects/samples studied by DIGE and those studied by ELISA. Clinical measures reflecting inflammatory activity including white blood cell count (WBC), hemoglobin (HB), platelets, erythrocyte sedimentation rate (ESR), and C-reactive protein (CRP) in FI and KD patients were described in Supplementary table 5.

Plasma preparation

For samples obtained at Stanford and UCSF, venous blood was collected in EDTA, heparin or citrate when blood was drawn for clinical laboratory determination of complete blood

count, differential and erythrocyte sedimentation rate. Within 2hrs of draw, whole blood samples were centrifuged at 25°C at 514 g for 5 minutes to remove cells and spun an additional two times at 4°C at 1730g for 5 and 15 minutes respectively to remove platelets. Processed plasma samples were stored at −80°C until analysis. No findings reported in this study could be attributed to differences in anticoagulant used (data not shown). Blood samples from SJIA, KD, and FI at UCSD were collected in EDTA and centrifuged within one hour to isolate plasma, which was stored at −80°C until analysis.

Sample preparation and protein labeling

To enrich samples for lower abundance plasma proteins, plasma samples were depleted of six of the abundant proteins (albumin, IgA, IgG, haptoglobin, transferrin, and alpha-1 antitrypsin) using Agilent Multiple Affinity Removal System (Agilent, Santa Clara, CA). Specifically, the depletion enabled the increased loading of the remaining proteins by fifteen-fold (data not shown). Depleted plasma was precipitated to separate proteins from detergents, salts, lipids, phenolics, and nucleic acids using a 2-D clean-up kit (GE Healthcare Biosciences, Pittsburgh, PA). Protease tablets (Roche Applied Science, Branford, CT) were dissolved as per manufacturer's instructions and applied as part of the buffer during the sample processing and 2-D clean-up processes. Protein concentrations were subsequently measured by protein microassay, using bovine serum albumin as a standard (Bio-Rad, Hercules, CA). Equal amounts of protein from paired F and Q samples were tagged with Cy3 or Cy5, respectively. Pooled standards were labeled with Cy2 and consisted of equal amounts of protein from all samples in the experiment. A 1 mM CyDye stock solution with dimethylformamide (DMF) was used. Supplementary Figure 2A showed the comparative DIGE analyses of the two SJIA patient plasma samples, before and after the protocol of Agilent column protein depletion, demonstrating the overall effectiveness of the DIGE analysis process and the efficiency of depleting the plasma top 6 most abundant proteins and enriching for less abundant proteins.

Two dimensional gel electrophoresis (2D DIGE)

Dye-labeled plasma protein samples were mixed with rehydration buffer (7M urea, 2M thiourea, 4% CHAPS, 0.0001% bromophenol blue) and pipetted across pH 3–10 NL BioRad Ready Strip IPG strips (Bio-Rad) inside a rehydration strip tray. Mineral oil was overlayed across each strip and the strip was rehydrated for 48 hours, after which protein samples were focused using Protean IEF focusing equipment at 200 volts for 10 hours, 500 volts for 2 hours, 1,000 volts for 2 hours, 5,000 volts for 2 hours, and 10,000 volts for 8 hours at 20°C.

Isoelectrofocused IPG strips were placed in SDS equilibration buffer (6M urea; 50mM Tris, pH 8.8; 30% glycerol, 2% SDS, 0.0002% bromophenol blue) for 15 minutes. IPG strips were subsequently loaded onto the second dimension gels, which contained 10% acrylamide, 375 mM Tris-Cl, pH 8.8, 0.05% APS, and 0.05% TEMED and were sealed by 1% agarose containing 2% SDS and 50mM Tris, pH 6.8. The second dimension of protein electrophoresis was performed using an ETTAN DALT vertical system with a current of 2 watts per gel for 16 hours at 10°C.

2D-DIGE analysis

Gels were imaged on the Typhoon 9400 Variable Mode Imager at specific wavelengths that excited Cy2, Cy3, or Cy5, allowing the protein profile of a given sample to be measured as soon as the second dimension was completed. Quantitative analysis was done on every spot on each gel using Progenesis software from Non-Linear USA Inc. (Durham, NC). Gel images went through a process of image quality assessment and were aligned to create protein spot index. We performed three sets of 2D-DIGE experiments: matched-pair F and Q from SJIA subjects (n=10), matched-pair F and Q from poly JIA subjects (n=5), and 12

KD/12 FI subjects with the pooled standards from each of the two previous experiments. The third experiment served as the bridge, allowing protein gel spot alignment, normalization and indexing across all assayed samples. Molecular weight and pI calibration were performed with Progenesis software using a set of protein spots with known MW and pI as internal standards.

Protein identification via MALDI-TOF/TOF mass spectrometry

Differentially expressed protein spots were excised from the gel using an Ettan Spot Picker (GE Healthcare Biosciences), digested with trypsin, spotted to a MALDI target and analyzed in MS and MS/MS modes with an Applied Biosystems (ABI) 4700 MALDI-TOF/TOF mass spectrometer. The identity of a subset of peptides detected was determined by searching MS/MS spectra against the Swiss-Prot database (June 10, 2008) restricted to human entries (15,720 sequences) using the Mascot (version 1.9.05; Matrix Science Inc., Boston, MA) search engine. Given that the MS and MSMS spectra are stored in an Oracle database (ABI schema version 3.19.0, data version 3.90.0), the ABI software GPS explorer and 4000 Series Explorer (V3.6, build 999) provide extensive Mascot integration. After the data acquisition, the spectra were processed to detect peaks using 4000 Series Explorer with the following parameter specified: peak detection - min S/N 3, local noise window width (m/z) 250, min peak width at full width half max(bins) 2.9; monoisotopic peaks - S/N threshold of 10. MSMS Mascot search parameters, including tryptic cleavage at only Lys or Arg, 2 of missed cleavages permitted, fixed modification of Carboxymethyl on Cys and variable modification of Oxidation on Met, were defined as part of an “Analysis” in GPS setup. Searches were restricted to 50 and 100 ppm for parent and fragment ions, respectively. Only b and y fragment ions were taken into account. We used Mascot default threshold of 5% probability that a protein identification is incorrect for accepting individual MSMS spectra. On completion of each search, the results are imported into the Oracle database and can be viewed and reported using the GPS Results Browser. In addition, an experienced mass spectroscopist reviewed all identification data before acceptance.

ELISA assays

ELISA assays were performed to measure plasma levels of selected proteins: serum amyloid A (SAA), S100A8, S100A9, S100A8/S100A9 complex (calprotectin), serum amyloid P (SAP), C-reactive protein (CRP), haptoglobin (HP), apolipoprotein A-1 (APO AI), alpha-2-macroglobulin (A2M) and S100A12. All assays, except for SAP and S1000A12, were performed using commercial ELISA kits: A2M, plasma was diluted 1:400 and assayed by AssayMax (St. Charles, MO) kit; APO A1, plasma was diluted 1:800 and assayed by AssayMax kit; S100A8 and S100A9, plasma was diluted 1:100 and assayed by kits from BMA Biomedicals (Augst, Switzerland); calprotectin, plasma was diluted 1:100 and assayed by Cell Sciences (Canton, MA) kit; CRP, plasma was diluted 1:250 and assayed by Immunology Consultants Laboratory (Newberg, OR) kit; HP, plasma was diluted 1:50,000 and assayed by Immunology Consultants Laboratory kit; SAA, plasma was diluted 1:50 and assayed by Antigenix America (Huntington Station, NY) kit; For SAP analysis, ELISA plates (MaxiSorp; Nunc, Rochester, NY) were coated with SAP antibody (Millipore, Billerica, MA) with PBS overnight at 4°C at 10 μg/ml. Plates were blocked with 1% bovine serum albumin (BSA) in phosphate buffered saline (PBS) (Sigma, St. Louis, MO) for 1hr at 37°C. Plates were washed and incubated with sample (diluted 1:1000) for 1hr at room temperature (RT) followed by another wash and subsequent incubation with anti-SAP rabbit antibody (Abcam, Cambridge, MA) diluted 1:100 with PBS plus 10% FBS, pH 7.0 for 1 hr at 37°C. Anti-rabbit horseradish peroxidase (HRP) (Southern Biotech, Birmingham, Alabama) diluted to 1:4000 was added for 30 minutes at 37 °C. For determination of S100A12, ELISA plates were coated with S100A12 antibody (Abcam) in carbonate buffer overnight at 4°C at 1μg/well. Plates were blocked with 0.25% BSA in PBS (Sigma) for 1hr

at 37°C. Plates were washed and incubated with sample (diluted 1:3) for 2 hrs at RT followed by another wash and subsequent incubation with biotin-conjugated anti-S100A12 antibody (R&D Systems, Minneapolis, MN) at 0.25 ug/well for 30 minutes at 37°C. Streptavidin conjugated to horseradish peroxidase (HRP) (Invitrogen, Carlsbad, CA) at 0.8 ug/ml in PBS was added for 30 minutes at 37°C. Substrate buffer followed by stop solution was added, and absorbance was read at 405 nm.

Statistical analyses

Patient demographic data was analyzed using "Epidemiological calculator" (R epicalc package). Hypothesis testing used Student t test and Mann-Whitney U test, and local FDR [24] to correct for multiple hypothesis testing issues. Nearest shrunken centroid (NSC) based feature selection, including permutation based FDR analysis, was performed using R PAM package [25]. Unsupervised heatmap analyses were performed using R stats package. Binary class clustering results were grouped into modified 2 × 2 contingency tables, which were used to calculate the proportion of the clustering results that agreed with clinical diagnosis and the statistical significance by the Fisher's exact test. Supervised linear discriminant analysis for binary (SJIA F vs Q, Poly JIA F vs Q) and three class (SJIA F, KD and FI) classifications, using R MASS package, led to the predictive linear discriminant analysis models. The predictive performance of each linear discriminant analysis model was evaluated by ROC curve analysis [26, 27]. The class prediction results from both the training and test data sets were grouped in modified 2 × 2 contingency tables and the statistical significance of the extent of agreement with clinical diagnosis was assessed by Fisher's exact test. Statistical test of correlation between DIGE and ELISA protein measurements was performed using R stats package.

RESULTS

Plasma protein profile distinguishes SJIA flare from quiescence

To determine the plasma protein profile associated with SJIA disease activity, we studied matched-pair plasma samples from 10 SJIA subjects at disease flare (F) and quiescence (Q). As expected, there were significant differences in laboratory values (leukocyte count, platelets, and sedimentation rate) and daily prednisone dose between the SJIA flare and quiescent samples (Supplementary Table 2A).

To prepare samples for 2D-DIGE, we depleted 6 abundant plasma proteins (see Materials and Methods), thereby enriching for lower abundance plasma proteins that are more likely to be biomarkers [28, 29]. We carried out 2D-DIGE on a mixture of equal amounts of protein from F and Q samples of each subject. Across all 10 gels, there were 889 plasma protein spots detected in the 2D-DIGE analyses. After normalization and manual review for candidate differentially expressed spots, we chose 96 protein features for identification by MALDI-TOF/TOF MS. Seven protein spots, representing hemoglobin and carbonic anhydrase from red blood cells, were removed from further analyses, leaving 89 identified protein features (Supplementary Figure 2, Supplementary Table 6). The MSMS protein identification analysis results were summarized in Supplementary Table 7 with SwissProt entry, Protein name, unique peptide detected, sequence coverage%, protein score, expectation value, molecular weight (MW) and pI.

To assess the association of disease status with expression patterns of these 89 protein spots, we used normalized volume data from the 20 SJIA samples and performed unsupervised hierarchical clustering analysis with heatmap plotting (Figure 1). The analysis shows 2 major clusters reflecting F and Q samples, indicating a flare "signature" in plasma. One F sample clustered with the Q branch. Clinical data suggested that the plasma protein

expression pattern reflected reduced disease activity in advance of clinically detectable improvement (see discussion). The Q samples formed 2 subclusters. Clinical and demographic data (age, ethnicity, treatment response to MTX, TNF, or IL1RA, steroid dependence, poly/monocyclic course, joint damage) from these 2 subclusters did not identify obvious differences between them. However, the subgroups differed in the length of time (number of days) since SJIA was active, consistent with the possibility that particular plasma proteins (e.g., apoA1, some haptoglobin species) normalize faster than others as disease is becoming quiescent.

Significant differences in SJIA flare versus quiescence patterns

Mass spectrometric identification revealed that the selected 89 protein spots represented 26 plasma proteins: alpha-1-antichymotrypsin (ACT), alpha-1-acid glycoprotein (AGP1), alpha-2-macroglobulin (A2M), inter-alpha-trypsin inhibitor light chain (AMBP), apolipoprotein A1 (APO A-I), apolipoprotein A-IV (APO A-IV), apolipoprotein D (APO D), apolipoprotein E (APO E), apolipoprotein L1 (APO L1), antithrombin III (ATIII), complement C3 (C3), complement C4 (C4), complement C9 (C9), C-reactive protein (CRP), fibrinogen β (FGB), fibrinogen γ (FGG), gelsolin (GSN), complement factor H (CFH), haptoglobin (HP), kininogenin (KLKB1), calgranulin A (S100A8/MRP8), calgranulin B (S100A9/MRP14), serum amyloid A (SAA), serum amyloid P (SAP), transthyretin (TTR), vitamin D binding protein (VDB). We determined the extent of F versus Q differences in levels of expression (normalized volumes) of the 89 spots using Student's t tests (Supplementary Table 6). The results indicate that F versus Q differences are statistically significant (P value < 0.05) for approximately 2/3 of the spots (59/89), representing 18 proteins and corroborating the generation of F and Q groups by cluster analysis of the 2D-DIGE data.

Optimization of the SJIA 2D-DIGE flare signature

To select the panel of features with strongest discriminating power between SJIA F and Q, we applied the nearest shrunken centroid (NSC) algorithm [25] to normalized volumes of the most discriminating spots (lowest P value in Supplementary Table 6) for each of the 26 proteins from the 2D-DIGE analysis. False discovery rate (FDR) analysis showed significant FDR increase with feature sets larger than 15 (Figure 2A, left). We used unsupervised clustering to analyze the top 15 protein spots (from TTR, CFH, APOA1, A2M, GSN, C4, AGP1, ACT, APOIV, SAP, HP, CRP, S100A8, S100A9 and SAA) as shown in the heatmaps in Figure 2B. These proteins demonstrated the ability to distinguish SJIA F and Q robustly. To assess the specificity of this panel, we tested its ability to distinguish poly JIA F versus Q. In contrast to the effective discrimination between SJIA F and Q ($P = 1.1 \times 10^{-4}$), the same protein spots discriminated poorly between poly JIA F and Q ($P = 0.5$). The panel discriminated SJIA F from FI ($P = 1.4 \times 10^{-4}$), but did not discriminate SJIA F from KD ($P = 0.19$). Thus, the specific plasma features that distinguish active from inactive SJIA can also distinguish SJIA from the more localized inflammation of poly JIA and from the milder inflammation associated with acute febrile illness, but not from the more aggressive systemic inflammation of KD.

ELISA-based SJIA flare biomarker panel

We were interested in whether the SJIA F panel could lead us to an immediate practical clinical tool, based on available antibodies and ELISA assays. We selected a panel of 9 of the 15 SJIA F (vs Q) proteins (SAP, SAA, S100A8, S100A9, HP, CRP, A2M, APO-A1, TTR) and the S100A8/S100A9 complex. We also included ATIII, which showed discriminating power in the 2D-DIGE (Supplementary Table 6) and S100A12, a protein of the S100 family found by other investigators to increase at SJIA flare (11; we confirmed the S100A12 association with SJIA F in our cohort by ELISA, data not shown). We performed

ELISA assays on a training set of samples, 12F/12Q (10/24 samples are matched from 5 subjects), and a test set, 10F/10Q (8/20 samples are matched from 4 subjects). Using data from these assays, we built classifiers with various subsets of the 12 ELISA assays. We sought to identify a biomarker panel of optimal feature number, balancing the need for small panel size, accuracy of classification, goodness of class separation (F vs Q), and sufficient sensitivity and specificity. Goodness of separation is defined by computing the difference (Δ) between discriminative scores, calculated as estimated probabilities [30]). When class is predicted correctly, Δ probability is the difference of the highest and next highest probability; when predicted incorrectly, Δ probability is the difference of the probability of the true class and the highest probability, which will be negative. Shown in Figure 3 are the SJIA F and Q box-whisker graphs. Boxes contain the 50% of values falling between the 25th and 75th percentiles; the horizontal line within the box represents the median value and the "whisker" lines extend to the highest and lowest values. The analysis revealed 7 to be the smallest panel size for which the "box" values of goodness of separation are positive for both SJIA F and Q, in both training and testing data sets. The 7-ELISA panel consists of A2M, APO-AI, CRP, HP, S100A8/S100A9, SAA, and SAP (Figure 4A). Shown in Supplementary Figure 3, the protein abundance of the SJIA marker proteins, quantified by either DIGE or ELISA assays, was described by the box-whisker graphs illustrating the distribution of measurement values across assayed SJIA, KD and FI samples. The trends for relative abundance of each biomarker across different clinical classes are consistent between DIGE and ELISA assays. We tested for correlation between the DIGE and ELISA measurements by Kendall's tau, which is a rank-based statistic. This revealed P = 0.02, indicating that ELISA and DIGE observations are statistically correlated, and therefore ELISA assays validate the DIGE observations.

To gauge the efficacy of the 7 ELISA panel as a classifier for SJIA disease activity, we performed linear discriminant analysis (Figure 4). This yielded 22/24 assignments that agree with clinical assessment in the training sample set and15/20 assignments that agree with clinical assessment in the test sample set (Figure 4A). The probabilities associated with these classification choices are plotted. The maximum estimated probability for each of the wrongly classified samples is marked with an arrow. As shown in Figure 4B, the 7 ELISA panel-based algorithm classified the training F samples with 91.6% agreement and the Q samples with 91.6% agreement with clinical class, with $P = 1.0 \times 10^{-4}$. With the test set data, the F samples were classified with 80% agreement and Q samples with 70% agreement with the clinical diagnosis, with $P = 0.07$. The misclassified patient in the SJIA Q training group was noted to flare clinically four weeks after her quiescent sample was drawn, and one of the misclassified subjects in the SJIA F test group was noted to be in clinical quiescence by his next visit, 2.5 months later. These findings again suggested that the classifier detects changes of disease state in advance of clinically detectable changes. Another misclassified subject in the SJIA F test group was noted to have concomitant (probable viral) gastroenteritis, raising the possibility that the classifier may distinguish fever and rash due to disease flare from that due to a viral or infectious process. Recalculation of *P* values for accuracy of classification, based on removing these 3 subjects, results in statistically significant values for both data sets (Figure 4B, $P^* = 9.6\times10^{-6}$; $P^* = 4\times10^{-3}$). A fourth misclassified SJIA F sample was from a subject with active arthritis without systemic systems, suggesting that the panel is weighted toward detection of activity of the systemic manifestations of SJIA.

For both training and test data sets, ROC analyses [26, 27] were performed to assess the performance of the SJIA flare classification algorithm. As ESR, CRP and S100A8/A9 are widely reported as possible measures of disease, we tested these markers either alone or in combination, in comparison to our own panel (Figure 4C). The ROC analyses yielded AUCs of 0.95 for our panel, ESR 0.96, S100A8/S100A9 0.73, CRP 0.82 with the training data set,

and with the test data set, our panel 0.82, ESR 0.86, S100A8/S100A9 0.78, CRP 0.65. The final classifier using observations from the combined training and test sets yielded AUCs for our panel of 0.94, ESR 0.92, S100A8/S100A9 0.74, CRP 0.72, and the panel of ESR-S100A8/A9-CRP 0.93 respectively. These analyses indicated that our panel was comparable to ESR for detection of flare, but better than either CRP or S100A8/S100A9 in SJIA F/Q discriminations.

Distinguishing SJIA flare from acute FI using ELISA panel

DIGE data indicated efficient discrimination between SJIA flare and the inflammation of acute FI (Figure 2B). We asked whether the ELISA panel would be sufficient to identify these clinical conditions. The levels of the biomarkers in 49 samples (including 22 SJIA F studied in Figure 4 and 27 new FI subjects) were measured by the 7 ELISA assays. Figure 5A plots the discriminant probabilities of the ELISA-based classifier for the assayed subjects. 16/22 SJIA F subjects were classified correctly as SJIA, and 25/27 FI samples were classified as FI. Fisher exact test of the 2×2 contingency tables of classification results yielded $P = 2.7 \times 10^{-6}$, indicating the effectiveness of biomarker-based classifier in discriminating SJIA F from FI. Similar results were obtained using 22 different SJIA F samples taken from the same subjects at different visits (not shown). Among the misclassified SJIA samples in Figure 5A are 3 SJIA F samples that are misclassified in Figure 4A and are discussed above. The efficacy of the ELISA panel as a classifier of SJIA versus acute febrile illness was further confirmed by comparative ROC analyses, which gave AUC values for the SJIA flare panel (0.838) that were higher than AUC values for S100A8/S100A9 (0.551), ESR (0.635) and CRP (0.571) alone (Figure 5B). These results support the potential clinical utility of the SJIA flare panel for separating SJIA F from the inflammation of acute FI.

Detection of impending flare with the SJIA flare ELISA panel

To test whether the ELISA-based biomarker panel has the capacity to detect “early” SJIA flare prior to clinically detectable disease activity, two sets of SJIA samples were compared: 5 SJIA quiescent samples (QF) drawn within 2–9 weeks prior to a clinical flare and samples from 10 SJIA quiescent controls (QQ), whose disease was quiet for 6 months before and after sample collection. All samples in this QQ and QF stratification analysis were different from those used in the previous analyses. ELISA data sets were used to develop a binary classifier (QQ versus QF). Figure 6A plots the classification results and shows that both QQ and QF samples have clear separation between the highest and next highest probability for the classifier assignment. Only one QF sample was misclassified and is marked with an arrow. Fisher exact test of the 2×2 contingency tables of classification results yielded $P = 3.7 \times 10^{-3}$, indicating the effectiveness of the classifier in prediction of impending SJIA flare. This was further confirmed by comparative ROC analyses, which gave AUC values of 0.90 for the SJIA flare panel, whereas other values were: ESR 0.68, S100A8/S100A9 0.74, CRP 0.82 (Figure 6B). These results support the potential clinical utility of the SJIA flare panel in predicting impending SJIA flare. With the small sample size and lack of an independent test sample set, however, this preliminary finding requires validation in further studies, powered with sufficient sample size.

Pathway analysis of the SJIA flare biomarkers

We analyzed the 15 proteins that are significantly differentially expressed in SJIA flare as a composite, using Ingenuity Pathway Analysis software (IPA version 7.6, Ingenuity Systems, Inc., Redwood City, CA). Strikingly, as shown in Figure 7, all 15 proteins are linked in one network by the software, with the central molecular driver identified as IL-1. Acute phase response signaling is identified as the top canonical pathway with a P value of 1.38×10^{-14}. To explore the possibility that a panel could be identified to directly distinguish SJIA F from

KD, the gel spots discriminating between SJIA F and KD with Student's t test P value < 0.05, were chosen for unsupervised heatmap analysis. A new panel of features from nine proteins (ATIII, A2M, HP, APOIV, GSN, APO A1, SAA, SAP, and AGP1) suggests that plasma profiles can identify 2 subsets of KD patients, one more similar to SJIA than the other (Figure 8A). This classifier uses different protein derivatives than the SJIA F vs Q panel, although 8 source proteins are shared. When the changes in these source proteins are analyzed by Ingenuity (Figure 8B), acute phase response signaling again is identified as the top canonical pathway function with P value = 2.34×10^{-8}.

DISCUSSION

Our initial 2D-DIGE results indicated differential plasma protein profiles between active and inactive SJIA. To our knowledge, this is the first study to describe a unique proteomic profile of SJIA F using 2D-DIGE. Because >50% of plasma protein content is accounted for by albumin and other abundant proteins, such as IgG and transferrin, we performed an initial depletion step, removing six of the most abundant proteins. This step allowed us to detect less abundant proteins, such as serum amyloid p [31]. The DIGE technique has a dynamic range of ~5 orders of magnitude in protein concentration [32], whereas plasma protein concentrations vary over ~10 orders of magnitude, with the highest concentrations reaching mgs/ml [33]. Even with the depletion step, protein detection by our 2D-DIGE system is limited to proteins whose plasma concentrations are >10 ug/ml, clearly influencing the composition of the SJIA flare signature we detected. In addition, potentially informative low molecular weight proteins may bind to albumin and thus be removed at the depletion step [34]. Nonetheless, as levels of some abundant plasma proteins are reduced (e.g., APO A-1, TTR) or increased (e.g. CRP) significantly during inflammatory states, and other proteins that are not found in normal control plasma rise to a level detectable by 2D-DIGE, such as S100A9, a flare signature is observable. Moreover, specific protein species are altered abundance during active SJIA and are sufficient to produce signatures that robustly differ from the protein pattern at SJIA quiescence and from other inflammatory conditions we tested (see more below).

From the 2-D DIGE, we evaluated 89 spots, representing 26 proteins, as candidate components of the SJIA F flare signature. Among these, some proteins have individually been associated with SJIA flare, such as SAA, CRP and the inflammation-associated S100A8/S100A9 complex [13, 35, 36]. In addition, our observation of reduced levels of APO A-1 at SJIA flare confirms previous investigations of JIA subjects [37]. The fact that these (expected) proteins were identified by our analyses increases confidence in the use of DIGE as a platform to detect plasma proteins differentially expressed in association with SJIA disease activity.

Particular isoforms/derivatives of 15 proteins gave rise to a robust SJIA flare signature that differentiated flare from quiescence and from acute febrile illnesses. These 15 proteins can be assigned to different functional groups, including proteins involved in the classical acute phase response, the innate immune system (S100 proteins), the complement cascade, the coagulation system and lipid/cholesterol metabolism. There is the substantial evidence supporting crosstalk between these pathways in inflammatory states. For example, CRP, a quintessential positive acute phase protein, binds molecular patterns typically found on the surface of pathogens and also activates the classical complement pathway [38, 39]. A2M, a thrombin (and other protease) inhibitor, is also a component of the innate immune system, acting as a scavenger of novel proteases introduced by pathogens [40]. APO A-1, the major protein component of high density lipoprotein (HDL), also has anti-inflammatory and anti-thrombotic properties [39, 41]. Acute phase HDL, where SAA is exchanged for APO A-1, are lipid transport particles, but also function in innate immune responses, for example, by

promoting monocyte chemotaxis [42]. APO A-IV, the major protein component of intestinal triacylglycerol-rich lipoproteins, is a positive acute phase protein involved in lipid homeostasis, but also reduces Toll-like receptor 4-induced pro-inflammatory cytokines [43, 44].

Our data show that the differentially expressed plasma proteins at SJIA F compared to Q have a substantial degree of specificity for SJIA F, compared to poly JIA F or FI; this is the case for both proteins detected by 2D-DIGE and by the ELISA panel. These observations are in line with other evidence indicating that specific patterns of acute phase reactants are associated with certain diseases [45–48]. In a relevant example, Yu et al [49] described a unique 2D protein fingerprint in KD versus non-KD febrile control subjects, with increases in protein spots, representing fibrinogen β and γ chains, α-1-antitrypsin, CD5 antigen-like precursor, and clusterin, and decreases in spots from immunoglobulin light chains. This pattern differs from SJIA flare, although we confirmed a significant difference in fibrinogen β between KD and FI, and noted a KD-specific increase in APO-D compared to FI subjects (Supplementary Table 6). Similarly, a study of gene expression in peripheral blood mononuclear cells (PBMC) showed that the list of genes differentially expressed in SJIA patients compared to controls had more overlap (35/286) with PBMC gene expression in an autoinflammatory condition (neonatal onset multisystem inflammatory disease, NOMID) than with PBMC gene expression in poly JIA (6/286) or KD (17/286) [50]. Disease-associated variation in acute phase proteins implies their independent regulation and is thought to reflect differences in the driving cytokines and their endogenous modulators [51]. This idea finds support within childhood rheumatic diseases in the apparent roles for IL-1β and IL-6 in SJIA, as compared to TNFα/sTNFR in poly JIA or interferon α in SLE [52–55].

Pathway analyses of the 15 proteins in the SJIA flare signature corroborate growing evidence implicating IL-1 as a key mediator of this disease. This is in line with recent findings that IL-1 beta is a central mediator of the arthritic matrix derived FSTL-1, which appears to be a biomarker of SJIA disease activity [56]. IL-1β and TNFα, pro-inflammatory cytokine products of monocyte/macrophages, are known to stimulate IL-6 production by monocyte/macrophages and endothelial cells. These cytokines, and IL-6 especially, act on hepatocytes to induce production of classical acute phase proteins, such as SAA and CRP, complement components and fibrinogen and suppress production of proteins such as APO A-1 [39]. Notably, the evidence of IL-1 activity, as reflected in the pattern of proteins in SJIA plasma at flare, is consistent with recent reports of the therapeutic effects of IL-1 inhibition in SJIA patients [52, 53].

Differences in profiles of PBMC transcripts or plasma proteins from active SJIA and acute KD are of particular interest because, at disease onset, these two conditions can present a diagnostic dilemma. Interestingly, two new molecular links appear, suggesting processes that differ between SJIA and at least a subset of KD subjects: IL-23, a cytokine associated with Th17 cells, and CD163, a scavenger receptor on alternatively activated macrophages, CD163 is known to bind and clear haptoglobin/hemoglobin complexes and monocyte/macrophages expressing this receptor have been implicated in SJIA, particularly in association with a life-threatening complication of the disease termed “macrophage activation syndrome” [57].

We detected a highly discriminatory SJIA flare signature by identifying the particular protein species (spot) most highly associated with disease activity. Different post-translational modifications, particularly altered glycosylation, and/or proteolysis of plasma proteins associated with active disease most likely underlie this observation [51, 58]. These changes are likely cytokine-driven. For example, it is known that matrix metallo-proteinases (MMPs), especially MMP-1, -3, -9 and -13 are induced by IL-1β [59, 60]. In a separate

study of low concentration plasma proteins, we have found that increased circulating MMP9 is associated with SJIA flare (Ling, XB et al, manuscript in preparation). More work is warranted to investigate the molecular events that generate specific protein modifications and intermediates in inflammatory states. Of note, increased levels of SAA-related derivatives are found in supernatants of IL-1β-activated human monocytes and are thought to reflect a block in SAA degradation [61]. These *in vitro* results are consistent with our observation of increased circulating levels of isoforms of SAA in SJIA flare. A biomarker panel based on the unique protein derivatives we identified as optimal for SJIA will require generation of specific detection reagents.

We validated a subset of our DIGE results using ELISA as an independent method. ROC curve analysis suggests that the 7 ELISA panel may aid in diagnosis of SJIA, as it was better than CRP or S100A8/9 at classifying SJIA versus acute FI. However, an important caveat is that the SJIA F subjects studied with our panel were not all new onset, untreated cases, which would be the best comparator group. The ELISA panel also might be useful to distinguish SJIA flare from inter-current infection in a febrile child with known SJIA. A prospective study with SJIA subjects will be required to address this potential clinical utility. Nonetheless, our panel appears to provide stronger classifying power than any single biomarker alone.

Our data suggest that certain changes in plasma protein profiles occur in advance of clinically detectable disease activity. In unsupervised analysis of our DIGE data, one SJIA F sample clustered with the Q samples. This subject had active disease at the time of sample draw, but entered clinical quiescence over the next 2 months. Based on the DIGE analysis, SAA had already normalized in the flare sample from this subject, suggesting this protein changes earlier than others. APO A-1 spots were also similar to a quiescent pattern; this protein may contribute to resolution of a flare by inhibiting monocyte activation and synthesis of pro-inflammatory cytokines [62]. The 7-member ELISA panel also classified 4 out of 5 quiescent samples correctly as “pre-flare”. This is in line with the previous observation of serum S100 protein level change in advance of clinical flare [63, 64], supporting the notion that disease flares can be predicted because local disease activity may be present before flares become clinically apparent. Larger studies are needed to determine whether the ELISA panel can reliably predict flare prior to clinically detectable disease activity. If so, it will be important to test the hypothesis that earlier treatment leads to a better short- or long-term outcome in SJIA.

In addition to the diagnostic challenges associated with fevers of unknown origin and fever in children with SJIA, prognostic challenges are prominent in SJIA. The clinical course is variable, ranging from a monocyclic episode with recovery in about 50% of subjects to a chronic, either polycyclic or persistent, condition, often with severe joint damage [6, 65]. Only subsets of SJIA patients respond to currently available therapies [66, 67]. Complications of SJIA include growth failure, macrophage activation syndrome and amyloidosis, the latter two being potentially life-threatening [68, 69]. Proteomic strategies provide an attractive approach to discover prognostic biomarkers in SJIA. We have found a preliminary suggestion that our ELISA panel may identify those subjects at onset who will have a monocyclic course (JLP, unpublished data). In this regard, it is encouraging that a recent 2D-DIGE analysis of synovial fluid provided evidence for markers that predict the transition from oligoarticular to polyarticular disease in a subset of oligoarticular-onset JIA subjects [32].

Supplementary Material

Refer to Web version on PubMed Central for supplementary material.

Acknowledgments

We would like to thank the subjects, families and medical staff of the Pediatric Rheumatology Clinics at Lucile Packard Children's Hospital at Stanford and at UCSF and the subjects, families and medical staff at UCSD for their participation in our study. This work was supported by the Dana Foundation, The Wasie Foundation, the Lucille Packard Foundation for Children's Health Initiative and the NIH. In addition, J.L. Park is supported by the American College of Rheumatology Research and Education Physician Scientist Development Award. She was also supported by Grant Number T32AR050942 from the National Institute of Arthritis and Musculoskeletal and Skin Diseases. The content is solely the responsibility of the authors and does not necessarily represent the official views of the National Institute of Arthritis and Musculoskeletal and Skin Diseases or the National Institutes of Health.

References

1. Weiss JE, Ilowite NT. Juvenile idiopathic arthritis. Pediatr Clin North Am. 2005; 52:413–442. vi. [PubMed: 15820374]
2. Singh-Grewal D, Schneider R, Bayer N, Feldman BM. Predictors of disease course and remission in systemic juvenile idiopathic arthritis: significance of early clinical and laboratory features. Arthritis Rheum. 2006; 54:1595–1601. [PubMed: 16645998]
3. Vastert SJ, Kuis W, Grom AA. Systemic JIA: new developments in the understanding of the pathophysiology and therapy. Best Pract Res Clin Rheumatol. 2009; 23:655–664. [PubMed: 19853830]
4. Schneider R, Laxer RM. Systemic onset juvenile rheumatoid arthritis. Bailliere's clinical rheumatology. 1998; 12:245–271. [PubMed: 9890097]
5. Wallace CA, Levinson JE. Juvenile rheumatoid arthritis: outcome and treatment for the 1990s. Rheumatic diseases clinics of North America. 1991; 17:891–905. [PubMed: 1767079]
6. Lomater C, Gerloni V, Gattinara M, Mazzotti J, et al. Systemic onset juvenile idiopathic arthritis: a retrospective study of 80 consecutive patients followed for 10 years. The Journal of rheumatology. 2000; 27:491–496. [PubMed: 10685819]
7. Calabro JJ, Holgerson WB, Sonpal GM, Khoury MI. Juvenile rheumatoid arthritis: a general review and report of 100 patients observed for 15 years. Seminars in arthritis and rheumatism. 1976; 5:257–298. [PubMed: 1251219]
8. Mottonen T, Hannonen P, Leirisalo-Repo M, Nissila M, et al. Comparison of combination therapy with single-drug therapy in early rheumatoid arthritis: a randomised trial. FIN-RACo trial group. Lancet. 1999; 353:1568–1573. [PubMed: 10334255]
9. Foell D, Wittkowski H, Hammerschmidt I, Wulffraat N, et al. Monitoring neutrophil activation in juvenile rheumatoid arthritis by S100A12 serum concentrations. Arthritis Rheum. 2004; 50:1286–1295. [PubMed: 15077313]
10. Wittkowski H, Frosch M, Wulffraat N, Goldbach-Mansky R, et al. S100A12 is a novel molecular marker differentiating systemic-onset juvenile idiopathic arthritis from other causes of fever of unknown origin. Arthritis Rheum. 2008; 58:3924–3931. [PubMed: 19035478]
11. Wittkowski H, Hirono K, Ichida F, Vogl T, et al. Acute Kawasaki disease is associated with reverse regulation of soluble receptor for advance glycation end products and its proinflammatory ligand S100A12. Arthritis Rheum. 2007; 56:4174–4181. [PubMed: 18050248]
12. Frosch M, Vogl T, Seeliger S, Wulffraat N, et al. Expression of myeloid-related proteins 8 and 14 in systemic-onset juvenile rheumatoid arthritis. Arthritis Rheum. 2003; 48:2622–2626. [PubMed: 13130482]
13. Frosch M, Ahlmann M, Vogl T, Wittkowski H, et al. The myeloid-related proteins 8 and 14 complex, a novel ligand of toll-like receptor 4: and interleukin-1beta form a positive feedback mechanism in systemic-onset juvenile idiopathic arthritis. Arthritis Rheum. 2009; 60:883–891. [PubMed: 19248102]
14. de Jager W, Hoppenreijs EP, Wulffraat NM, Wedderburn LR, et al. Blood and synovial fluid cytokine signatures in patients with juvenile idiopathic arthritis: a cross-sectional study. Ann Rheum Dis. 2007; 66:589–598. [PubMed: 17170049]
15. Jelusic M, Lukic IK, Tambic-Bukovac L, Dubravcic K, et al. Interleukin-18 as a mediator of systemic juvenile idiopathic arthritis. Clin Rheumatol. 2007; 26:1332–1334. [PubMed: 17597334]

16. Miyamae T, Malehorn D, Lemster B, Mori M, et al. Serum protein profile in systemic-onset juvenile idiopathic arthritis differentiates response versus nonresponse to therapy. Arthritis research & therapy. 2005; 7:R746–755. [PubMed: 15987476]
17. Sobieska M, Fassbender K, Aeschlimann A, Bourgeois P, et al. Still's disease in children and adults: a distinct pattern of acute-phase proteins. Clin Rheumatol. 1998; 17:258–260. [PubMed: 9694067]
18. Chen DY, Chen YM, Ho WL, Chen HH, et al. Diagnostic value of procalcitonin for differentiation between bacterial infection and non-infectious inflammation in febrile patients with active adult-onset Still's disease. Ann Rheum Dis. 2009; 68:1074–1075. [PubMed: 19435724]
19. Eberhard OK, Haubitz M, Brunkhorst FM, Kliem V, et al. Usefulness of procalcitonin for differentiation between activity of systemic autoimmune disease (systemic lupus erythematosus/systemic antineutrophil cytoplasmic antibody-associated vasculitis) and invasive bacterial infection. Arthritis Rheum. 1997; 40:1250–1256. [PubMed: 9214425]
20. Delevaux I, Andre M, Colombier M, Albuisson E, et al. Can procalcitonin measurement help in differentiating between bacterial infection and other kinds of inflammatory processes? Ann Rheum Dis. 2003; 62:337–340. [PubMed: 12634233]
21. Burns JC, Glode MP. Kawasaki syndrome. Lancet. 2004; 364:533–544. [PubMed: 15302199]
22. Petty R, Southwood T, Manners P, Baum J, et al. International League of Associations for Rheumatology classification of juvenile idiopathic arthritis: second revision, Edmonton, 2001. The Journal of rheumatology. 2004; 31:390–392. [PubMed: 14760812]
23. Sandborg C, Holmes T, Lee T, Biederman K, et al. Candidate early predictors for progression to joint damage in systemic juvenile idiopathic arthritis. The Journal of rheumatology. 2006; 33:2322–2329. [PubMed: 16960920]
24. Efron B, Tibshirani R, Storey J, Tusher V. Empirical bayes analysis of microarray experiment. Journal of the American statistical association. 2001; 96:1151–1160.
25. Tibshirani R, Hastie T, Narasimhan B, Chu G. Diagnosis of multiple cancer types by shrunken centroids of gene expression. Proceedings of the National Academy of Sciences of the United States of America. 2002; 99:6567–6572. [PubMed: 12011421]
26. Zweig MH, Campbell G. Receiver-operating characteristic (ROC) plots: a fundamental evaluation tool in clinical medicine. Clin Chem. 1993; 39:561–577. [PubMed: 8472349]
27. Sing T, Sander O, Beerenwinkel N, Lengauer T. ROCR: visualizing classifier performance in R. Bioinformatics. 2005; 21:3940–3941. [PubMed: 16096348]
28. Jacobs JM, Adkins JN, Qian WJ, Liu T, et al. Utilizing human blood plasma for proteomic biomarker discovery. J Proteome Res. 2005; 4:1073–1085. [PubMed: 16083256]
29. Roche S, Tiers L, Provansal M, Seveno M, et al. Depletion of one, six, twelve or twenty major blood proteins before proteomic analysis: the more the better? J Proteomics. 2009; 72:945–951. [PubMed: 19341827]
30. Tibshirani R, Hastie T, Narasimhan B, Chu G. Diagnosis of multiple cancer types by shrunken centroids of gene expression. Proc Natl Acad Sci U S A. 2002; 99:6567–6572. [PubMed: 12011421]
31. Huang H-L, Stasyk T, Morandell S, Mogg M, et al. Enrichment of low-abundant serum proteins by albumin/immunoglobulin G immunoaffinity depletion under partly denaturing conditions. Electrophoresis. 2005; 26:2843–2849. [PubMed: 15971195]
32. Gibson DS, Blelock S, Curry J, Finnegan S, et al. Comparative analysis of synovial fluid and plasma proteomes in juvenile arthritis--proteomic patterns of joint inflammation in early stage disease. J Proteomics. 2009; 72:656–676. [PubMed: 19367684]
33. Anderson N. The human plasma proteome: history, character, and diagnostic prospects. Mol Cell Proteomics. 2002; 1:845–867. [PubMed: 12488461]
34. Tirumalai RS, Chan KC, Prieto DA, Issaq HJ, et al. Characterization of the low molecular weight human serum proteome. Mol Cell Proteomics. 2003; 2:1096–1103. [PubMed: 12917320]
35. De Beer FC, Mallya RK, Fagan EA, Lanham JG, et al. Serum amyloid-A protein concentration in inflammatory diseases and its relationship to the incidence of reactive systemic amyloidosis. Lancet. 1982; 2:231–234. [PubMed: 6124669]

36. Wu JF, Yang YH, Wang LC, Lee JH, et al. Comparative usefulness of C-reactive protein and erythrocyte sedimentation rate in juvenile rheumatoid arthritis. Clinical and experimental rheumatology. 2007; 25:782–785. [PubMed: 18078633]
37. Tselepis AD, Elisaf M, Besis S, Karabina SA, et al. Association of the inflammatory state in active juvenile rheumatoid arthritis with hypo-high-density lipoproteinemia and reduced lipoprotein-associated platelet-activating factor acetylhydrolase activity. Arthritis Rheum. 1999; 42:373–383. [PubMed: 10025933]
38. Black S, Kushner I, Samols D. C-reactive Protein. J Biol Chem. 2004; 279:48487–48490. [PubMed: 15337754]
39. Dayer E, Dayer J-M, Roux-Lombard P. Primer: the practical use of biological markers of rheumatic and systemic inflammatory diseases. Nature Reviews Rheumatology. 2007; 3:512–520.
40. Armstrong PB, Quigley JP. Alpha2-macroglobulin: an evolutionarily conserved arm of the innate immune system. Dev Comp Immunol. 1999; 23:375–390. [PubMed: 10426429]
41. Yui Y, Aoyama T, Morishita H, Takahashi M, et al. Serum prostacyclin stabilizing factor is identical to apolipoprotein A-I (Apo A-I). A novel function of Apo A-I. Journal of Clinical Investigation. 1988; 82:803–807. [PubMed: 3047170]
42. Navab M, Anantharamaiah GM, Fogelman A. The role of high-density lipoprotein in inflammation. Trends in cardiovascular medicine. 2005; 15:158–161. [PubMed: 16099381]
43. Khovidhunkit W, Duchateau P, Medzihradszky K, Moser A, et al. Apolipoproteins A-IV and A-V are acute-phase proteins in mouse HDL. Atherosclerosis. 2004; 176:37–44. [PubMed: 15306172]
44. Recalde D, Ostos MA, Badell E, Garcia-Otin AL, et al. Human apolipoprotein A-IV reduces secretion of proinflammatory cytokines and atherosclerotic effects of a chronic infection mimicked by lipopolysaccharide. Arterioscler Thromb Vasc Biol. 2004; 24:756–761. [PubMed: 14751811]
45. Braunwald E. Biomarkers in heart failure. N Engl J Med. 2008; 358:2148–2159. [PubMed: 18480207]
46. Kawachi-Takahashi S, Tanaka K, Takahashi M, Kawashima T, Shimada K. Determination of serum C9 level by immunodiffusion. Elevation in patients with infectious or allergic skin diseases. International archives of allergy and applied immunology. 1975; 48:161–170. [PubMed: 46851]
47. Kawachi-Takahashi S, Takahashi M, Kogure M, Kawashima T. Letter: Elevation of serum C9 level associated with Behcet disease. The Japanese journal of experimental medicine. 1974; 44:845–847. [PubMed: 4215915]
48. Bene L, Fust G, Fekete B, Kovacs A, et al. High normal serum levels of C3 and C1 inhibitor, two acute-phase proteins belonging to the complement system, occur more frequently in patients with Crohn's disease than ulcerative colitis. Digestive Diseases and Sciences. 2003; 48:1186–1192. [PubMed: 12822883]
49. Yu H-R, Kuo H-C, Sheen J-M, Wang L, et al. A unique plasma proteomic profiling with imbalanced fibrinogen cascade in patients with Kawasaki disease. Pediatric allergy and immunology. 2009; 20:699–707. [PubMed: 19170925]
50. Ogilvie E, Khan A, Hubank M, Kellam P, Woo P. Specific gene expression profiles in systemic juvenile idiopathic arthritis. Arthritis and rheumatism. 2007; 56:1954–1965. [PubMed: 17530721]
51. Gabay C, Kushner I. Acute-phase proteins and other systemic responses to inflammation. N Engl J Med. 1999; 340:448–454. [PubMed: 9971870]
52. Pascual V, Allantaz F, Arce E, Punaro M, Banchereau J. Role of interleukin-1 (IL-1) in the pathogenesis of systemic onset juvenile idiopathic arthritis and clinical response to IL-1 blockade. The Journal of experimental medicine. 2005; 201:1479–1486. [PubMed: 15851489]
53. Yokota S, Imagawa T, Mori M, Miyamae T, et al. Efficacy and safety of tocilizumab in patients with systemic-onset juvenile idiopathic arthritis: a randomised, double-blind, placebo-controlled, withdrawal phase III trial. Lancet. 2008; 371:998–1006. [PubMed: 18358927]
54. Prince FH, Twilt M, Ten Cate R, Van Rossum MA, et al. Long-term follow-up on effectiveness and safety of etanercept in JIA: the Dutch national register. Annals of the rheumatic diseases. 2008
55. Pascual V, Farkas L, Banchereau J. Systemic lupus erythematosus: all roads lead to type I interferons. Current opinion in immunology. 2006; 18:676–682. [PubMed: 17011763]

56. Wilson DC, Marinov AD, Blair HC, Bushnell DS, et al. Follistatin-like-protein-1 is a mesenchyme-derived inflammatory protein and may represent a biomarker for systemic-onset juvenile rheumatoid arthritis. Arthritis Rheum. 2010
57. Fall N, Barnes M, Thornton S, Luyrink L, et al. Gene expression profiling of peripheral blood from patients with untreated new-onset systemic juvenile idiopathic arthritis reveals molecular heterogeneity that may predict macrophage activation syndrome. Arthritis Rheum. 2007; 56:3793–3804. [PubMed: 17968951]
58. Wu W, Wang G, Baek S, Shen R-F. Comparative study of three proteomic quantitative methods, DIGE, cICAT, and iTRAQ, using 2D gel- or LC-MALDI TOF/TOF. Journal of proteome research. 2006; 5:651–658. [PubMed: 16512681]
59. Ge X, Ma X, Meng J, Zhang C, et al. Role of Wnt-5A in interleukin-1beta-induced matrix metalloproteinase expression in rabbit temporomandibular joint condylar chondrocytes. Arthritis and rheumatism. 2009; 60:2714–2722. [PubMed: 19714632]
60. Lin C-C, Kuo C-T, Cheng C-Y, Wu C-Y, et al. IL-1 beta promotes A549 cell migration via MAPKs/AP-1- and NF-kappaB-dependent matrix metalloproteinase-9 expression. Cellular signalling. 2009; 21:1652–1662. [PubMed: 19616091]
61. Migita K, Yamasaki S, Shibatomi K, Ida H, et al. Impaired degradation of serum amyloid A (SAA) protein by cytokine-stimulated monocytes. Clinical and experimental immunology. 2001; 123:408–411. [PubMed: 11298127]
62. Hyka N, Dayer JM, Modoux C, Kohno T, et al. Apolipoprotein A-I inhibits the production of interleukin-1beta and tumor necrosis factor-alpha by blocking contact-mediated activation of monocytes by T lymphocytes. Blood. 2001; 97:2381–2389. [PubMed: 11290601]
63. Foell D, Wulffraat N, Wedderburn LR, Wittkowski H, et al. Methotrexate withdrawal at 6 vs 12 months in juvenile idiopathic arthritis in remission: a randomized clinical trial. JAMA. 2010; 303:1266–1273. [PubMed: 20371785]
64. Schulze zur Wiesch A, Foell D, Frosch M, Vogl T, et al. Myeloid related proteins MRP8/MRP14 may predict disease flares in juvenile idiopathic arthritis. Clin Exp Rheumatol. 2004; 22:368–373. [PubMed: 15144135]
65. Sandborg C, Holmes TH, Lee T, Biederman K, et al. Candidate early predictors for progression to joint damage in systemic juvenile idiopathic arthritis. The Journal of rheumatology. 2006; 33:2322–2329. [PubMed: 16960920]
66. Wallace C, Huang B, Bandeira M, Ravelli A, Giannini E. Patterns of clinical remission in select categories of juvenile idiopathic arthritis. Arthritis and rheumatism. 2005; 52:3554–3562. [PubMed: 16255044]
67. Gattorno M, Piccini A, Lasiglié D, Tassi S, et al. The pattern of response to anti-interleukin-1 treatment distinguishes two subsets of patients with systemic-onset juvenile idiopathic arthritis. Arthritis and rheumatism. 2008; 58:1505–1515. [PubMed: 18438814]
68. Woo P. Systemic juvenile idiopathic arthritis: diagnosis, management, and outcome. Nature clinical practice rheumatology. 2006; 2:28–34.
69. Sawhney S, Woo P, Murray KJ. Macrophage activation syndrome: a potentially fatal complication of rheumatic disorders. Archives of Disease in Childhood. 2001; 85:421–426. [PubMed: 11668110]

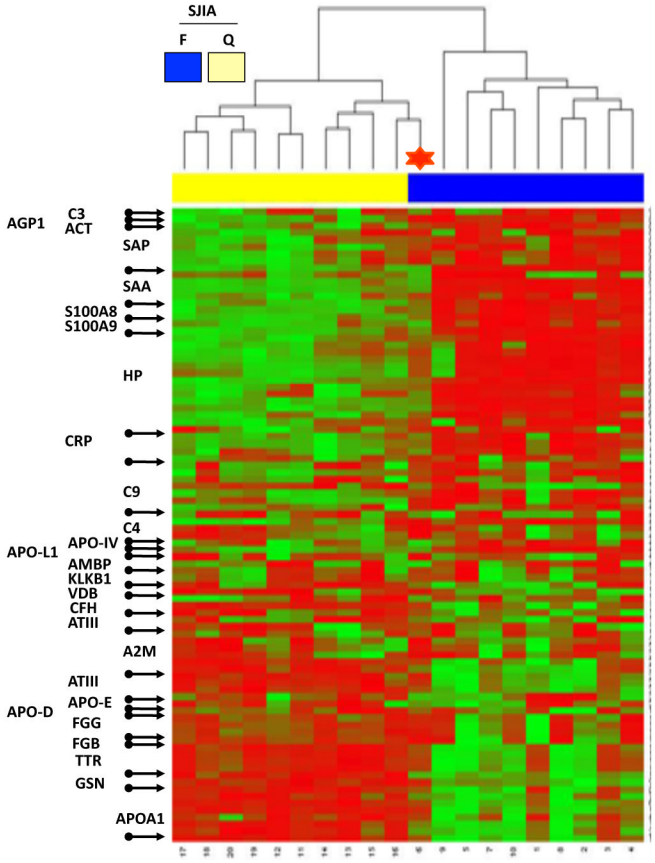

Figure 1.

Heatmap display of unsupervised hierarchical clustering of the relative protein abundance (normalized volume data, low-green and high-red) in paired SJIA F/Q plasma samples. The rows of heatmap represent the 89 gel spots derived from 26 different proteins (labeled with SwissProt protein names at the left of the heatmap) with each column of that row representing a different sample from subjects with SJIA flare (blue) and SJIA quiescence (yellow). The SJIA F sample, clustered with the SJIA Q branch, is labeled with a red star.

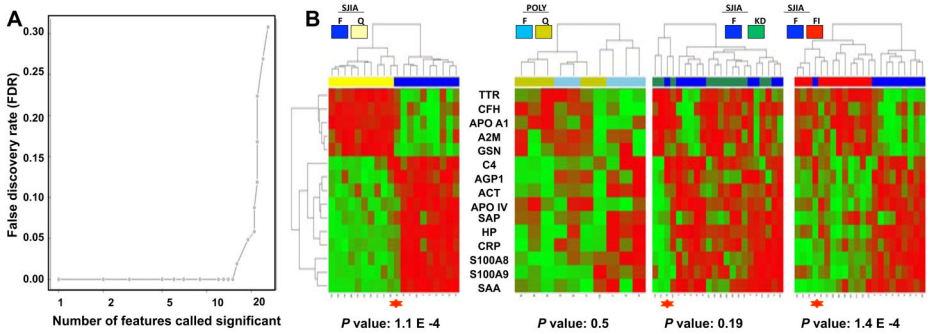

Figure 2.

Construction of robust SJIA flare panel. A. False discovery rate (FDR) analysis of the 26 proteins discriminating SJIA F and Q. X-Y plot of FDR as a function of the number of proteins called significant. B. Heatmap display of unsupervised clustering analyses of expression of the top 15 proteins, ranked by the nearest shrunken centroid algorithm (NSC), in SJIA F/Q, Poly JIA F/Q, SJIA F/KD, SJIA F/FI samples. The misclassified SJIA F sample (Figure 1) is labeled with a red star in each heatmap.

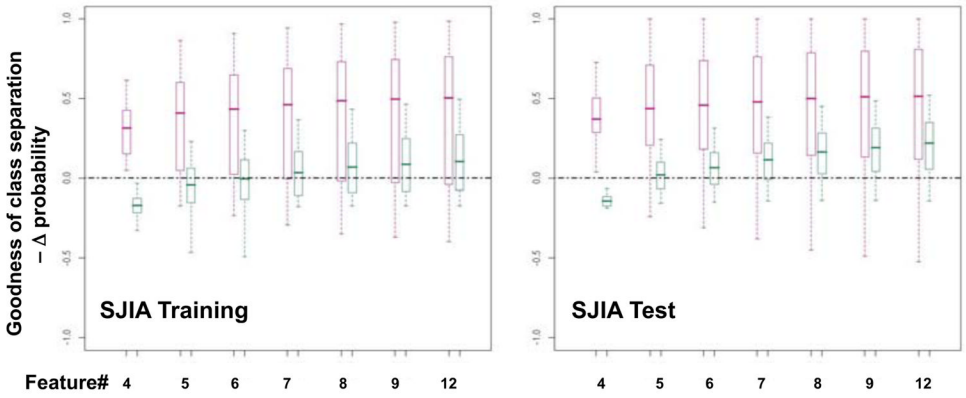

Figure 3.

Selection of 7 ELISA bioimarker panel and validation of DIGE results. A. Goodness of separation analysis to select optimal biomarker panel size for the SJIA flare ELISA analysis. Using ELISA data from SJIA F/Q training and test data sets, as indicated, various classifiers of different panel size (feature #) were tested for their goodness of separation between flare (red) and quiescence (green) as shown by the box-whisker graphs. Boxes contain the 50% of values falling between the 25th and 75th percentiles; the horizontal line within the box represents the median value and the "whisker" lines extend to the highest and lowest values. B. ELISA assays validate biomarker observations from DIGE assays. The box-whisker graphs illustrate the spread of the protein abundance of each biomarker from SJIA F/Q, KD and FI samples using either DIGE or ELISA assays. Boxes contain the 50% of values falling between the 25th and 75th percentiles; the horizontal line within the box represents the median value and the "whisker" lines extend to the highest and lowest values.

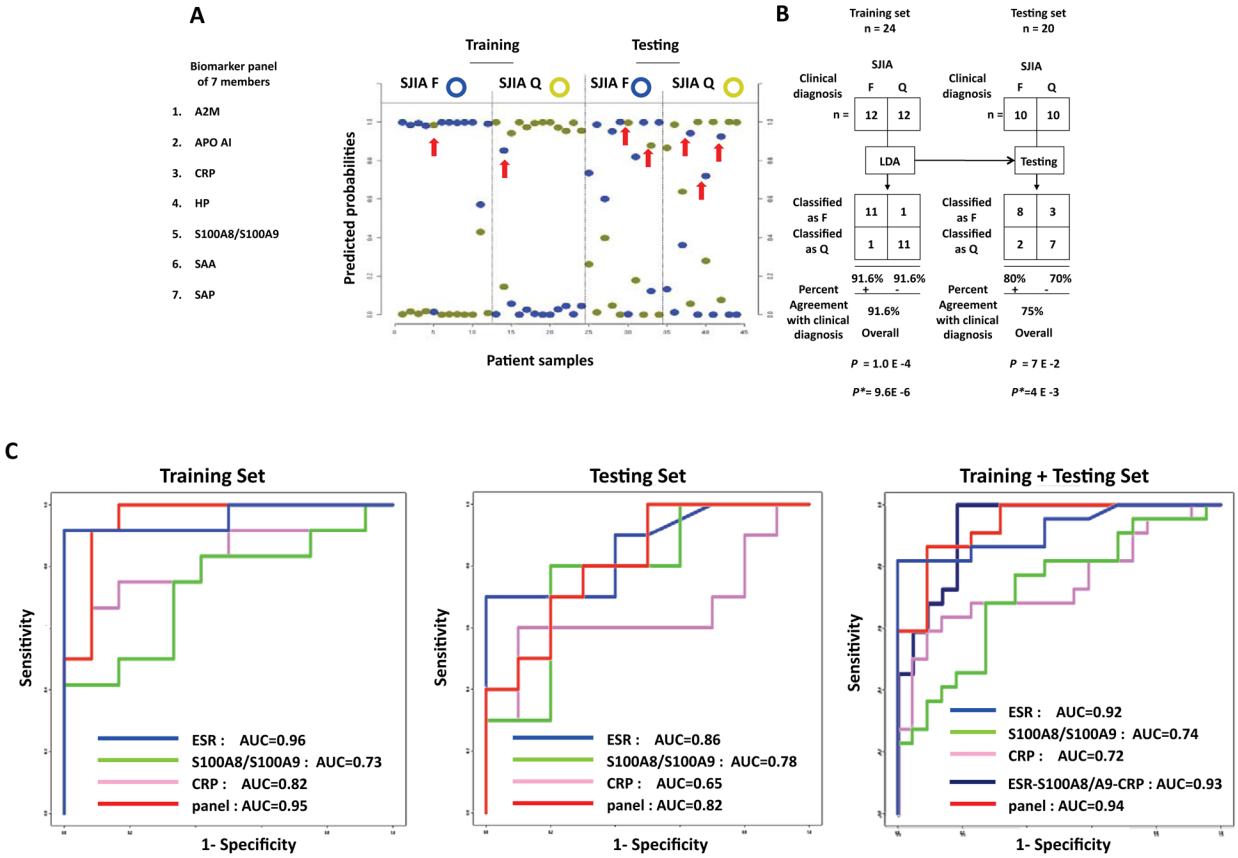

Figure 4.

Linear discriminant analysis of the ELISA-based SJIA flare biomarker panel differentiating SJIA F from Q samples. A. SJIA flare biomarker panel of 7 ELISA assays. Linear discriminant analysis (LDA) was performed with training data from SJIA F (n=17) and Q (n=17) samples evaluated with the biomarker panel. Estimated probabilities for the training (left) and test data (right) are plotted. Samples are partitioned by the true class (upper) and predicted class (lower). The maximum estimated probability for each of the wrongly assigned samples is marked with a red arrow. The trained LDA model was tested using an independent data set from SJIA F (n=10) and Q (n=10) samples. B. The classification results from training and test sets are shown as 2×2 contingency tables. Fisher exact test was used to measure *P* values of the 2×2 tables with (upper) and without (lower) confounding F samples. C. ROC analyses, using training, test or combined training and testing data sets, to compare the SJIA F and Q classification performance by either ESR, S100A8/S100A9, CRP, the panel of ESR-S100A8/A9-CRP, or SJIA flare ELISA panel, respectively.

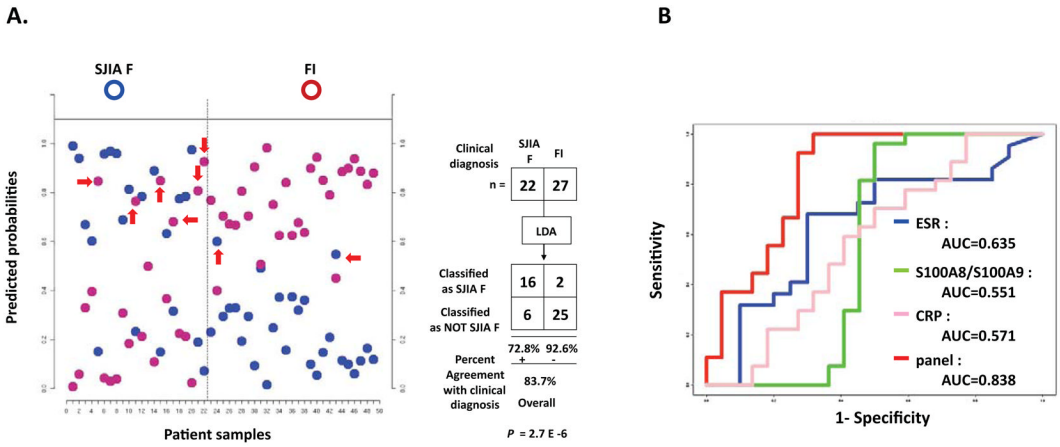

Figure 5.

Linear discriminant analysis of the 7-protein SJIA flare biomarker panel, differentiating SJIA F from FI subjects. (A) LDA analysis. SJIA F (n=22) and FI (n=27) subjects were used to develop a binary-class classifier. Samples are partitioned by the true class (upper) and predicted class (lower). The maximum estimated probability for each of the wrongly assigned samples is marked with a red arrow. The LDA classification results are shown as a 2×2 contingency table. Fisher exact test was used to measure the statistical significance (*P* value) of the 2×2 table. B. ROC analyses. The effectiveness of the biomarker panel to discriminate SJIA F from FI was compared to either S100A8/S100A9, CRP or ESR respectively.

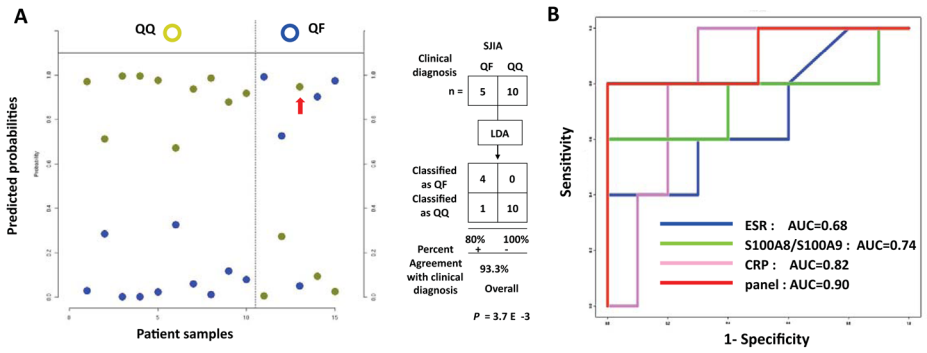

Figure 6.

Linear discriminant analysis of the ELISA-based SJIA flare biomarker panel in detection of impending SJIA flare. QF: 10 SJIA quiescent samples drawn within 2–9 weeks of a clinical flare; QQ: 10 SJIA quiescent controls who remained in quiescence for 6 months after the sample was drawn. A. Estimated probabilities for the training (left) and test data (right). Samples are partitioned by the true class (upper) and predicted class (lower). The maximum estimated probability for each of the wrongly assigned samples is marked with a red arrow. SJIA QQ and QF samples were used as training set to develop a binary classifier. The classification results are shown as a 2×2 contingency table, comparing SJIA QF to QQ. Fisher exact test was used to measure the *P* value of the 2×2 table. B. ROC analyses, using training data sets to compare the SJIA F and Q classification performance by ESR, S100A8/S100A9, CRP or SJIA flare panel.

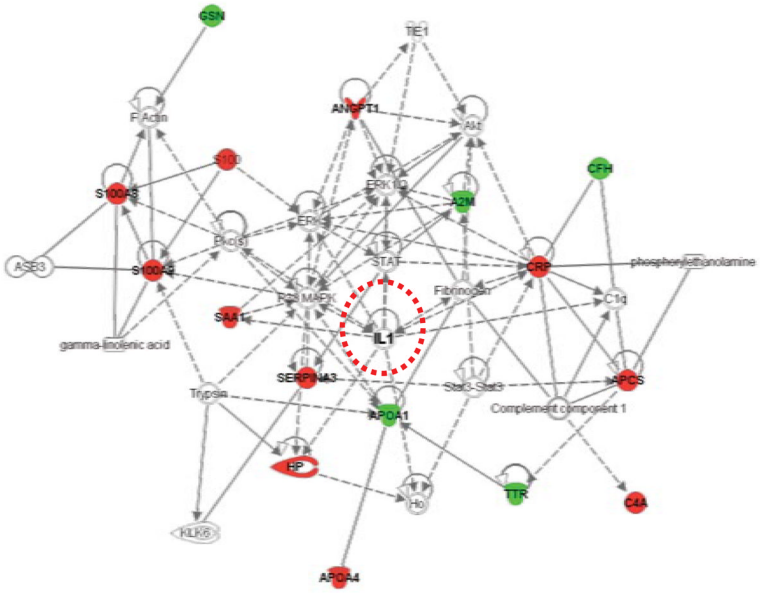

Figure 7.

Pathway analysis of the proteins in the SJIA signature. Data mining software (Ingenuity Systems, www.ingenuity.com, CA) was used with differentially (F vs Q) expressed plasma proteins to identify gene ontology groups and relevant canonical signaling pathways associated with SJIA flare. The intensity of the node color indicates the degree of up- (red) or down- (green) regulation in SJIA F. Nodes are displayed using shapes that represent the functional class of the gene product and different relationships are represented by line type (see key). Relationships are primarily due to co-expression, but can also include phosphorylation/dephosphorylation, proteolysis, activation/deactivation, transcription, binding, inhibition, biochemical modification.

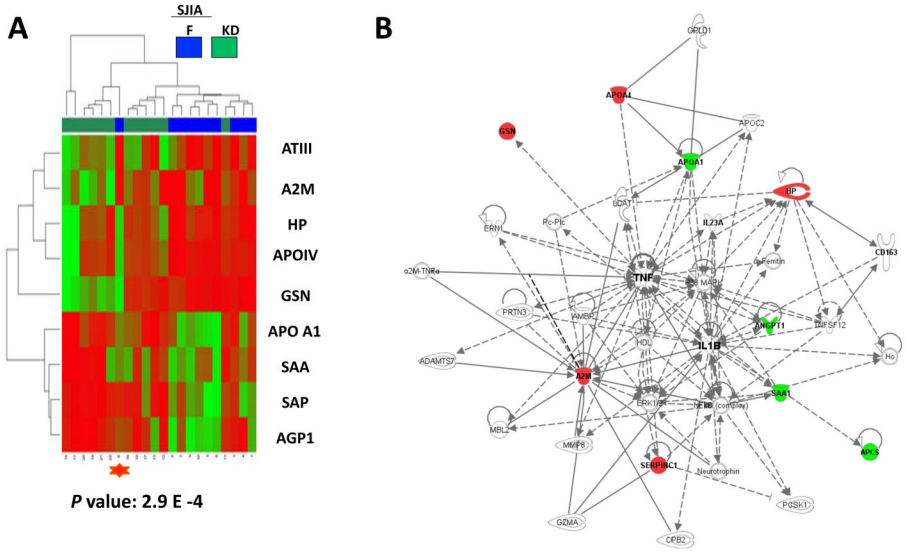

Figure 8.

Analysis of the protein profiles differentiating SJIA F from KD subjects. A. Heatmap display of unsupervised clustering analyses of expression of the top 9 proteins with Student's t test *P* value < 0.05 comparing SJIA F and KD samples. The mis-clustered SJIA F sample (shown in Figure 1 labeled with a red star) by the SJIA F panel when comparing SJIA F to either SJIA Q or FI is also mis-clustered when comparing SJIA F and KD (labeled with a red star). B. Data mining software (Ingenuity Systems, www.ingenuity.com, CA) was used with differentially (SJIA F vs KD) expressed plasma proteins to identify gene ontology groups and relevant canonical signaling pathways associated with SJIA flare. The intensity of the node color indicates the degree of up- (red) or down- (green) regulation in SJIA F. Nodes are displayed using shapes that represent the functional class of the gene product and different relationships are represented by line type (see key). Relationships are primarily due to co-expression, but can also include phosphorylation/dephosphorylation, proteolysis, activation/deactivation, transcription, binding, inhibition, biochemical modification.